

# The Effect of Nb Content on Microstructure Evolution of GH4169 superalloy During Hot Deformation

Wen Chen <sup>1</sup>, Peng Zhang <sup>1</sup>, Jing Xie <sup>1</sup>, Yang Liu <sup>1</sup> and Wenxia Zhao <sup>2,\*</sup>

<sup>1</sup>China National Erzhong Group Deyang Wanhang Die Forging Co., LTD., Deyang 618000, Sichuan, China

<sup>2</sup>AECC Beijing Institute of Aeronautical Materials, Beijing 100095, China

**Abstract:** This research conducted a thermal compression deformation test on two GH4169 alloy samples with 5.40wt% and 5.21wt% Nb contents respectively, under deformation temperatures ranging from 900°C to 1030°C and the strain rates of 0.04s<sup>-1</sup>, 0.08s<sup>-1</sup>. Data from the deformation test were used to study the effects of deformation temperature and strain rate on the microstructure,  $\delta$  phase morphology, and  $\delta$  phase evolution of both alloy samples, so as to reveal the structural evolution mechanism. The results show that the long needle-like  $\delta$  phase in the alloy microstructure with high Nb content undergoes deformation fracture and decomposition fracture during deformation and compression under high temperature, with the fracture decomposition temperature being 990°C. Moreover, microstructures of alloys with low Nb content were dominated by granular  $\delta$  phases; as the deformation temperature increases or the strain rate decreases, the content of the  $\delta$  phase gradually decreases, causing the alloy's dynamic recrystallization grain size and dynamic recrystallization volume fraction to gradually increase from deformation twins at low temperatures to complete recrystallization at high temperatures.

**Keywords:** GH4169 superalloy, Nb content,  $\delta$  phase, Hot deformation, dynamic recrystallization

## 1. Introduction

GH4169 is a nickel-iron-based superalloy used at medium and high temperatures. It is an important material for aero-engine turbine discs[1-3]. Since turbine disks work under high temperatures and in high-stress environments, it is essential to ensure high-temperature strength and high resistance to low cycle fatigue to obtain a uniform and fine microstructure[4-8]. Generally, turbine disks are manufactured through multi-stage thermal deformation processes, and it is difficult to obtain a fine microstructure through satisfactory recrystallization and less grain growth. In GH4169 alloy, the body-centered tetragonal  $\gamma''$  phases (Ni<sub>3</sub>Nb) are the main strengthening phases, supplemented by the face-centered cubic structure  $\gamma'$  (Ni<sub>3</sub>AlTi), and  $\delta$  phases of the orthogonal structure (Ni<sub>3</sub>Nb). The structure and properties of GH4169 alloy are very sensitive to the hot working process. Improper process control will cause coarse and mixed crystals, which will affect the long-lasting notch sensitivity, the toughness of the forging, etc.

The mechanical properties of GH4169 are very sensitive to the changes in microstructure, while the microstructure of the alloy is directly affected by the chemical composition[9-12]. The addition of Nb not only affects the GH4169 alloy's  $\gamma''$  phases, i.e., the strengthening phases, but also affects the  $\delta$  phases. According to existing research, given that the Nb element content is 4.80wt%,

and the static complete resolubilization temperature of  $\delta$  phase is 990°C, but when the Nb element content is close to 5.50wt%, the static complete resolubilization temperature of the  $\delta$  phase exceeds 1,030°C. Because the  $\delta$  phases in GH4169 alloy can hinder the growth of grains by pinning the grain boundaries, a suitable temperature needs to be selected as the pretreatment temperature for large forgings. Maintaining a good microstructure state of the forging billet is the basis for preparing a turbine disk with excellent performance, and the selection of the temperature is mainly based on the patterns of dissolution and re-dissolution of the  $\delta$  phases.

At present, research has been conducted on the dissolution behavior of  $\delta$  phases during high-temperature deformation of GH4169 alloy, but there is no in-depth discussion on the evolution mechanism of  $\delta$  phases during deformation and the effect of  $\delta$  phase evolution on the high-temperature deformation mechanism of alloy[13,14]. In particular, the number of research conducted on the effect of Nb element content on the changes of alloy microstructure during deformation remains scarce[15,16]. Systematically studying the evolution process and structural characteristics of the  $\delta$  phases in alloys with different Nb element contents is not only important for offering formulation guidance in the hot working process of GH4169 alloys, but also for providing a theoretical basis for the precise control of deformation structure and performance.

\* Corresponding author: [wenxia.zhao@outlook.com](mailto:wenxia.zhao@outlook.com)

## 2. Experimental Procedures

### 2.1 Materials and Methods

In this study, the material used was an alloy forging bar made from Fushun special steel with a diameter of 220 mm. Two contents of the Nb element were selected, and the chemical compositions (wt%) of the alloys are as shown in Table 1. A thermal simulation test sample was cut along the circumferential direction (equal radius) and machined into  $\phi 10\text{mm} \times 15\text{mm}$ .

**Table 1** Chemical composition of test sample (wt%)

Element	C	Ni	Cr	Nb	Mo	Ti	Al	Mn	Si	B	Fe
HNB	0.03	54.2	18.3	5.4	2.9	0.9	0.5	0.08	0.06	0.00	Ba
	0.00	0.0	2.1	5.1	6.5	2.6	0.0	0.0	0.0	0.05	l
LNB	0.03	54.1	18.1	5.2	2.9	0.9	0.5	0.08	0.07	0.00	Ba
	0.00	8.3	3.0	5.0	8.5	4.0	0.0	0.0	0.05	l	

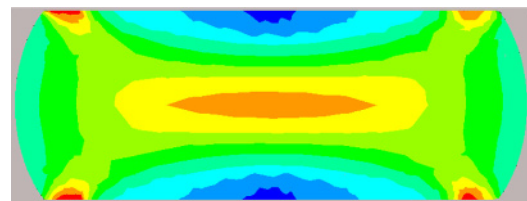
The thermal compression test was carried out on the computer-controlled Gleeble-1500 thermal simulation test machine. Both ends of the specimen were lubricated with high-temperature glass lubricant. The deformation temperatures selected were 900°C, 930°C, 960°C, 990°C, 1020°C, the strain rates were 0.04 s<sup>-1</sup>, 0.08 s<sup>-1</sup>, and the strain exerted was 50%. After the sample was compressed to the status of the specified amount of strain, it was quickly water quenched to retain its high-temperature deformation structure. The compressed sample was cut along the axial direction using wire EDM, and then corroded with a mixed solution of 50mL H<sub>2</sub>O + 40mL HCl + 10mL HF after performing mechanical polishing. The microstructure was observed using OLYMPUS GX51 optical microscope and NanoNova450 scanning electron microscope.

### 2.2 The Effect of Deformation Temperature on Microstructure

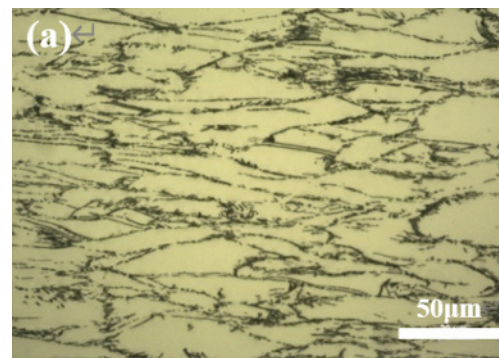
The cross section of the deformed sample is shown in Figure 1, as can be seen that the deformation and temperature of core area is higher than edge area, and microstructure of the core area can reflect the real state under high temperature.

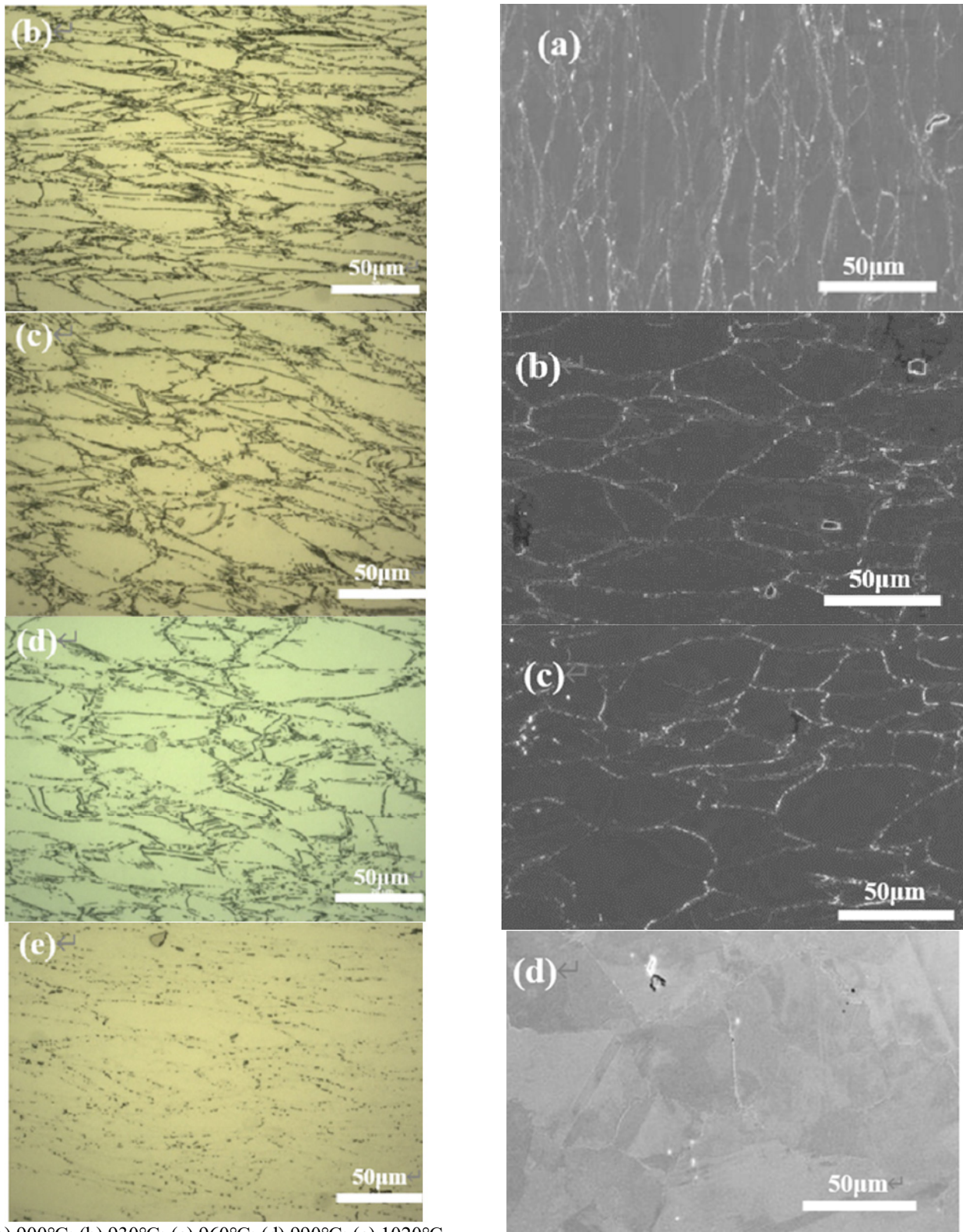
At 0.04 s<sup>-1</sup> strain rate, 50% deformation, the volume fractions of the  $\delta$  phases at the heart of the high-Nb-content alloy (HNB) were about 17.8%, 16.6%, 14.3%, 7.6%, and 0.67% respectively; the volume fractions of the  $\delta$  phases at the heart of the low Nb content alloy (LNB) were about 3.8%, 1.9%, 1.6%, 0.2%, 0%, respectively. Microstructure of specimen during hot deformation at different temperature were shown in Fig. 2 and Fig. 3. Zhang and Wang et al. [17,18] found that during high-temperature thermal compression and deformation, since the  $\delta$  phases and the matrix  $\gamma$  phases are in a non-coherent relationship, it is not easy for moving dislocations to cut the  $\delta$  phases, and the cutter tends to bend and bypass the  $\delta$  phases. Also, the  $\delta$  phases in the test alloy nucleate at the grain boundary and appear mainly in the form of short

rods/long strips. During deformation, for the short rod-shaped  $\delta$  phases, the movement dislocation occurs mainly via the bypass mechanism, but for clusters/long strip  $\delta$  phases, it is difficult for moving dislocations to bypass and advance, causing an instance of piling up to occur near the  $\delta$  phases, resulting in stress concentration. When the stress reaches the fracture limit of the  $\delta$  phase, the cluster/long strip  $\delta$  phases decomposes and fractures. Cai et al. [19] found that long strip  $\delta$  phases show dissolution fracture when studying the static dissolution behavior of the  $\delta$  phases. The reason is that under high-temperature conditions, a relatively large tension is generated on the interface between the phase and the matrix, which destroys the original interface stress balance, and creates grooves at the interface. Compared with the plane, the curvature radius of the curved surfaces on both sides of the groove is smaller, while the phases at the groove curved surface can be preferentially dissolved, which destroys the interfacial tension balance. To maintain balance, the groove needs to be further deepened, and this process needs to be repeated until the  $\delta$  phases dissolve and break [20]. It can be seen that during compression deformation, the strain applied from the outside increases the subgrain boundary or high-density dislocation area inside the long strip  $\delta$  phases, which in turn leads to the deformation and fracture of the  $\delta$  phases. meanwhile, a large amount of moving dislocations accumulate near the long needle-shaped  $\delta$  phases, and under the effect of the dislocation stress field, a fast path is provided for the diffusion of niobium atoms in the  $\delta$  phases, while the accelerated diffusion of niobium promotes the dissolution and fracture of the long strip  $\delta$  phases during the deformation process. It is precisely due to the combined effect of deformation fracture and dissolution fracture that the long needle-like  $\delta$  phases spheroidize and decompose during high-temperature compression and deformation, transforming themselves into granular  $\delta$  phases.



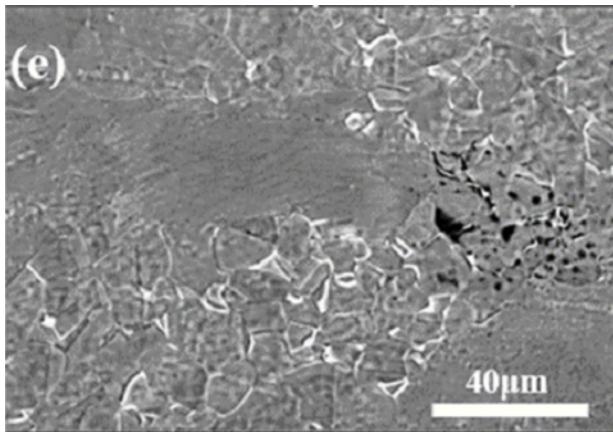
**Figure 1.** Cross-sectional schematic diagram





(a) 900°C; (b) 930°C; (c) 960°C; (d) 990°C; (e) 1020°C

**Figure 2.** Fiber structure of HNB samples at different temperatures under the deformation rate of  $0.04\text{s}^{-1}$



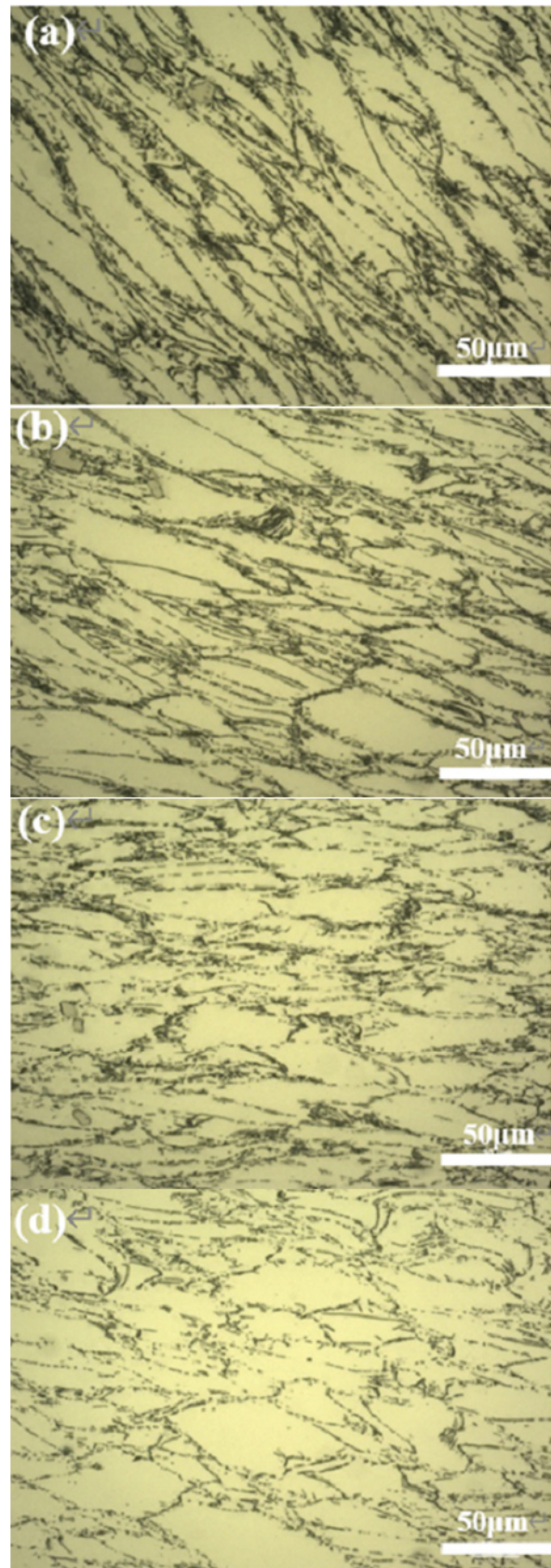
(a) 900°C; (b) 930°C; (c) 960°C; (d) 990°C; (e) 1020°C

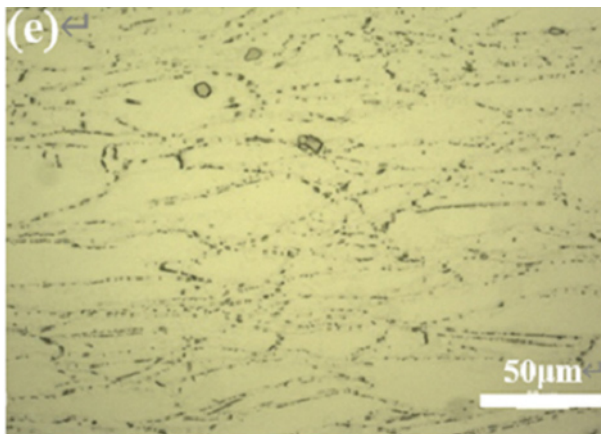
**Figure 3.** Fiber structure of LNB samples at different temperatures under the deformation rate of  $0.04s^{-1}$

### 2.3 The Effect of Strain Rate on Microstructure

After deformation at 990°C and under different strain rates, the microstructures of GH4169 alloy are similar were shown in Fig.4 and Fig.5, which are showing equiaxed grains formed by recrystallization, most of the long strip  $\delta$  phases are obviously bent, twisted or broken, deformed and fractured, as well as dissolved and fractured, in addition to the obvious appearance of strip-like structures along the direction of applied force. However, in the microstructure deformed at the low strain rate, the content of the unbroken long strip  $\delta$  phases is lesser than that at the high strain rate, the content of granular  $\delta$  phases is larger, and the structure is more uniform, indicating that a low strain rate is conducive to the formation of a good deformed structure. The reason is that under deformation at high temperature, a low strain rate can prolong the deformation process, so that the dislocation cross slip and diffusion climbing process can be fully carried out, which is conducive to the progress of dynamic recrystallization and the decomposition as well as spheroidization of the long strip  $\delta$  phases, thereby forming a uniform deformed structure.

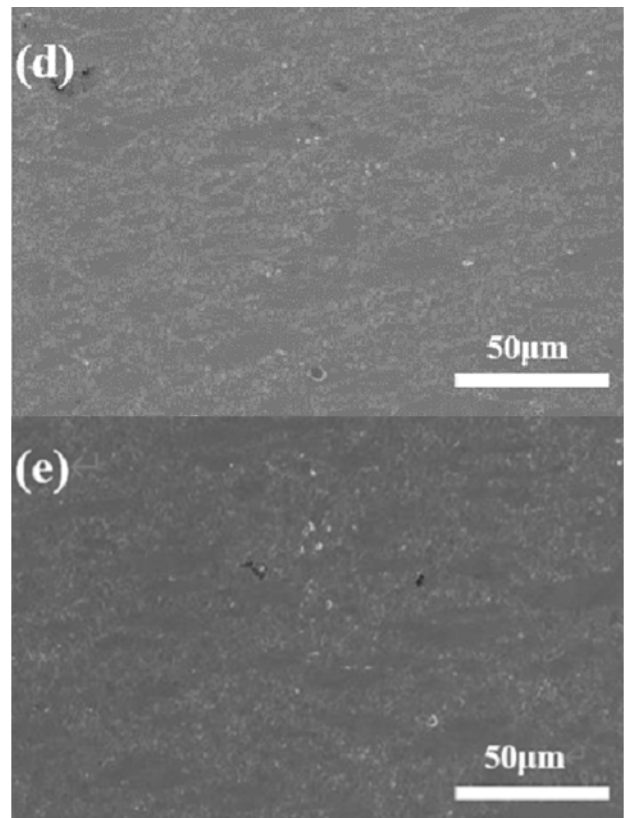
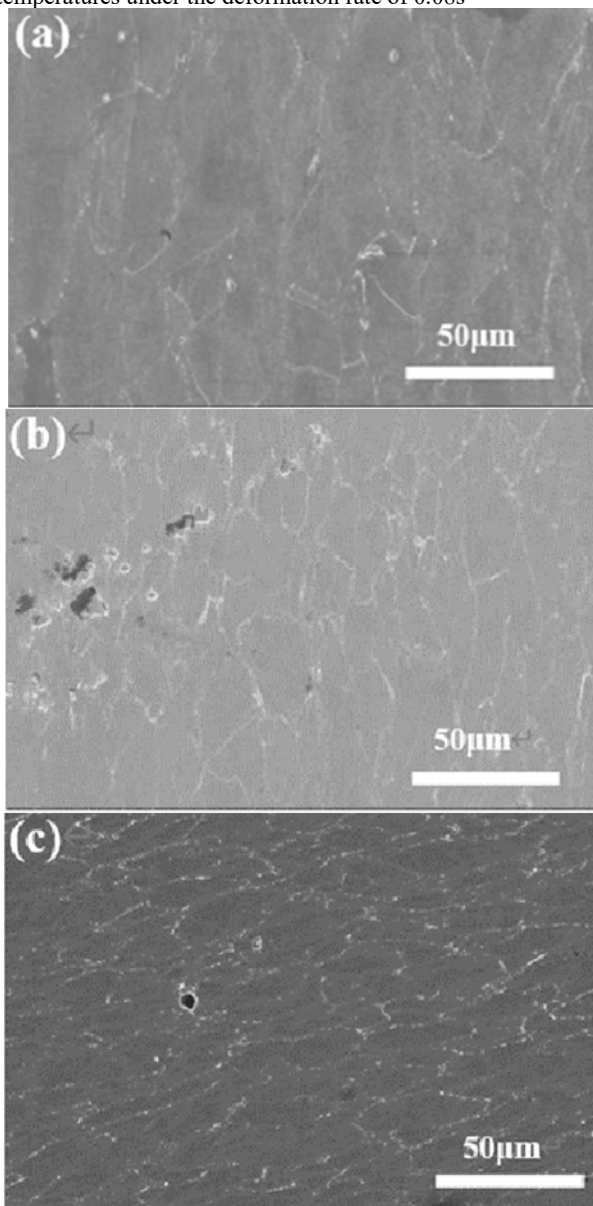
The content of  $\delta$  phases in GH4169 alloy with high Nb content gradually decreases, but the  $\delta$  phases are not completely re-dissolved until 1020°C and are distributed as discontinuous particles on the grain boundary, increasing the dynamic recrystallization grain size of the alloy from ASTM 7.5 to ASTM 7.0. the  $\delta$  phases in the low Nb content GH4169 alloy are generally re-dissolved at 990°C, and the dynamic recrystallization grain size of the alloy grows from ASTM7.5 to ASTM6.0.





(a) 900°C; (b) 930°C; (c) 960°C; (d) 990°C; (e) 1020°C

**Figure 4.** Fiber structure of HNB samples at different temperatures under the deformation rate of  $0.08s^{-1}$



(a) 900°C; (b) 930°C; (c) 960°C; (d) 990°C; (e) 1020°C

**Figure 5.** Fiber structure of LNB samples at different temperatures under the deformation rate of  $0.08s^{-1}$

### 3. Conclusion

(1) There are a large number of clusters/long strip  $\delta$  phases distributed in the microstructure of the high Nb content GH4169 alloy. Due to the combined effects of deformation fracture and dissolution fracture during high-temperature compression deformation, the long strip  $\delta$  phases are bent, twisted, and folded until spheroidization.

(2) The  $\delta$  phases in the microstructure of the low Nb content GH4169 alloy are mainly forged rod-like/granules. With the increase of temperature, the short rod-like  $\delta$  phases spheroidize and decompose, while the granular  $\delta$  phases are re-dissolved, and the  $\delta$  phases are completely re-dissolved at 1,020°C.

(3) With the increase of deformation temperature or decrease of strain rate, the content of  $\delta$  phases in GH4169 alloy with high Nb content gradually decreases, but the  $\delta$  phases are not completely re-dissolved until 1020°C and are distributed as discontinuous particles on the grain boundary, increasing the dynamic recrystallization grain size of the alloy from ASTM 7.5 to ASTM 7.0.

(4) With the increase of the deformation temperature or the decrease of the strain rate, the  $\delta$  phases in the low Nb content GH4169 alloy are generally re-dissolved at 990°C, and the dynamic recrystallization grain size of the alloy grows from ASTM7.5 to ASTM6.0.

## References

1. Kennedyrl. Allvac® 718plus TM , superalloy for the next forty years[C]. Superalloys 2005. Warrendale , PA: TMS, 2005:1–14 .
2. Sundararaman M, Mukhopadhyay P, Banerjee S. Precipitation of the  $\delta$ -Ni<sub>3</sub>Nb phase in two nickel base superalloys[J]. Metall Trans, A 1988;19A:453–65.
3. Collier JP, Wong SH, Phillips JC, Tien JK. The effect of varying Al, Ti, and Nb content on the phase stability of Inconel 718[J]. Metall Trans, A 1988;19A:1657–65.
4. Dix AW, Hyzak JM, Singh RP. Application of ultra fine grain alloy 718 forging billet[C]. Superalloys 1992. Warrendale, PA: TMS; 1992. p. 23–32.
5. Ruiz C, Obabueki A, Gillespie K. Evaluation of the microstructure and mechanical properties of Delta processed alloy 718[C]. Superalloys 1992. Warrendale, PA: TMS; 1992. p. 33–42.
6. Zhang Yun, Huang Xuebing, Wang Yong, et.al. Delta phase and deformation fracture behavior of Inconel 718 alloy[C]. Superalloys 718, 625, 706 and Various Derivatives Edited by E.A. Loria. Warrendale , PA: TMS ,1997:229–236.
7. Saied Azadian, Liu-Ying Wei, Richard Warren. Delta phase precipitation in Inconel 718[J]. Materials Characterization, 2004; 53:7–16.
8. Y. Desvallées, M. Bouzidi, F. bois, et al. Delta phase in Inconel 718: Mechanical properties and forging process requirements[J]. Superalloys 718,625,706 and Various Derivatives Edited by B.A. Loria. The Minerals, Metals&Materials Society, 1994.
9. S. Mahadevan, S. Nalawade, J. B. Singh, et al. Evolution of  $\delta$  phase microstructure in alloy 718[J]. 7th International Symposium on superalloy 718 and derivatives. Edited by: E.A. Ott, J. R. Groh, A Banik, I, Dempster, T. P. Gabb, R, Helmink. TMS-2010.
10. H. Yuan, W. C. Liu. Effect of the  $\delta$  phase on the hot deformation behavior of Inconel 718[J]. Materials Science and Engineering A 408 (2005) 281–289.
11. Hongjun Zhang, Chong Li, Qianying Guo. Delta precipitation in wrought Inconel 718 alloy; the role of dynamic recrystallization [J]. Materials Characterization, 133 (2017) 138–145.
12. Cai DY, Zhang WH, Nie PX, Liu WC, Yao M. Dissolution kinetics and behavior of phase in Inconel 718[J]. Trans Nonferrous Met Soc China 2003; 13(6):1338–1341.
13. Schafrik RE, Ward DD, Groh JR. Application of alloy 718 in GE aircraft engines: past, present and next five years[C]. Superalloys 718, 625, 706 and various derivatives. Warrendale, PA: TMS; 2001. p. 1–11.
14. Wang Y, Zhen L, Shao WZ, Yang L, Zhang XM. Hot working characteristics and dynamic recrystallization of delta-processed superalloy 718[J]. J Alloy Compd 2009;44:341–346.
15. K. Wang, M.Q. Li, J. Luo, et al. Effect of the  $\delta$  phase on the deformation behavior in isothermal compression of superalloy GH4169[J]. Materials Science and Engineering A 528 (2011) 4723–4731.
16. Thomas A, El-Wahabi M, Cabrera JM, Prado JM. High temperature deformation of Inconel 718[J]. J Mater Process Technol 2006;177:469–72.
17. Zhang. H. Y, Zhang H, Cheng. M,et al. Deformation characteristics of  $\delta$  phase in the delta-processed Inconel 718 alloy [J]. Materials Characterization, 61 (2010) 49-53 .
18. Cone FP. Observations on the development of delta phase in IN718 alloy[C]. Superalloys 718, 625, 706 and various derivatives. PA: TMS; 2001. p. 323–332.
19. Cai DY, Zhang WH, Liu WC, Yao M. Dissolution behavior of  $\delta$  phase in Inconel 718[J]. Journal of Iron and Steel Research, 14; 2002. p. 61–64. (in Chinese).
20. Si Jia-Yong, Chen Long, Liao Xiao-hang, et al. Microstructure Evolution of Delta-Processed GH4169 Alloy during Hot Deformation[J]. Materials For Mechanical Engineering, 2017 , 41 (4): 6–10. (in Chinese).